Magnetotransport studies of the single and bilayer two dimensional electron gas in the quantum Hall regime

Galistu, G.M.

Publication date
2010

1. Introduction

1.1 The classical Hall effect

In 1879 Edwin Hall discovered that the application of a magnetic field B perpendicular to a thin conducting slab through which a current flows produces a voltage across the slab and perpendicular to the current (*Fig.1*). This voltage has been called the Hall voltage V_H and the effect itself is called the Hall effect.

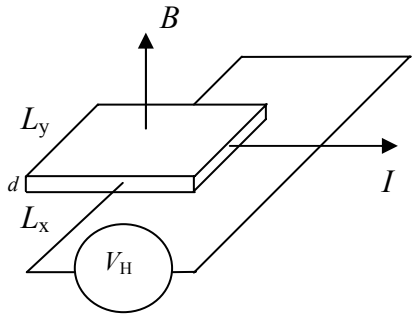

Figure 1.1 Schematic representation of the classical Hall effect.

So basically the Hall voltage is caused by the Lorentz force acting on the charges moving in the presence of a magnetic field. In equilibrium the Lorentz force $|F_L| = qv_DB$ is balanced by the electric force qV_H/L_y, where q is the carrier charge, v_D is the drift velocity and L_y is the width of the sample. So $V_H = v_DBL_y$ exhibits a linear dependence on the magnetic field B. Writing the current I as the product of the drift velocity v_D, the charge density n_q and the cross-sectional area of the sample $S = L_yd$, we find the perpendicular resistivity $R_H = V_H/I$ to be [1]

$$R_H = \frac{B}{qn_ed} = \frac{B}{qN_S}, \tag{1.1}$$

where $n_e = n_q/q$ is the number of carriers per unit volume and N_S is the number of carriers per unit surface area. Because the Hall resistance R_H only depends on the magnetic field B and the carrier density and not on other material parameters, the Hall effect has become a standard tool of material characterization. The direct proportionality of the Hall resistivity on the local magnetic field has allowed the development of scanning Hall probe microscopes which allow for instance a detailed determination of the magnetic field distribution near the vortices in type II superconductors [2]. The ordinary Hall effect can be fully explained by classical ideas about electron transport in metals, like the Drude model and the semi-classical theories elaborated in *Refs*. [3-5]. The fact that there is a quantum mechanical follow-up in the form of the quantum Hall effect which adds totally new dimensions to the study of low dimensional electronic systems, originally came as a complete surprise in physics as a whole.

1.2 The quantum Hall effect

The discovery of the ordinary Hall effect and advent of the quantum Hall effect (K. von Klitzing, 1980) are one century apart. The quantum Hall effect has already led to two Nobel prizes in physics, one for the integral quantum Hall effect [6] in 1985 and one for the fractional quantum Hall effect [7-9] in 1998. These robust quantum phenomena on a macroscopic scale Hall effect manifest themselves in the transport parameters of the two dimensional electron gas that are directly measurable, notably the longitudinal resistance (usually denoted by R_{xx} or R_0) and the Hall resistance (usually denoted by R_{xy} or R_H).

Still to date, more than 25 years after the first discovery, our microscopic understanding of the quantum Hall effect is far from being complete. The quantum Hall effect is standard observed in strong perpendicular magnetic fields B and at low temperatures ($T \leq$ 4 K) and it is well known that the phenomenon only exists because of the breaking of translational invariance by random impurities. Instead of the linear dependence of R_H with varying magnetic field B, it now turns out that the Hall resistance is quantized in units of h/e^2

$$R_H = \frac{h}{ie^2} \approx \frac{25.8128}{i} k\Omega \quad . \tag{1.2}$$

Here, i is an integer, h denotes Planck's constant and e is the charge of the electron. It is now generally accepted that the transitions between adjacent quantum Hall plateaus are continuous *quantum phase transitions* that are characterized by a diverging length scale ξ

usually termed the *localization length* of the electrons near the Fermi energy. The longitudinal resistance R_0 shows a peak at the transitions but it vanishes at the plateau values of R_H. The quantization phenomenon is extraordinarily accurate (better than one part in 10^8 [10]). This precision led the International Committee for Weights and Measures (CIPM) to adopt the quantum Hall effect as the new standard for electrical resistance in 1988.

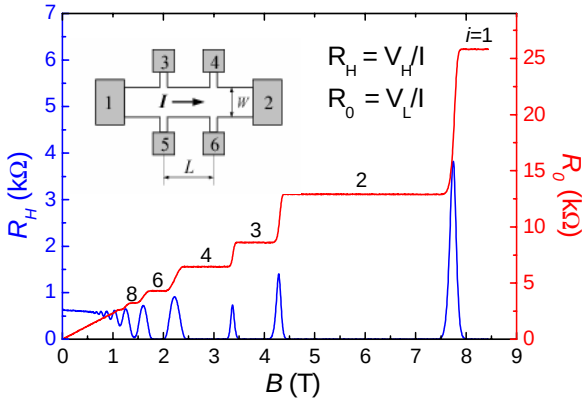

Figure 1.2 Quantum Hall effect measured on a sample with Hall bar geometry (top left corner). The Hall voltage V_H is measured between contacts 3 and 5 or 4 and 6. The longitudinal voltage V_L is measured between contacts 3 and 4 or 5 and 6. Data taken on an InGaAs/GaAs quantum well with electron density $n_e = 2.7 \times 10^{15}$ m^{-2} at T = 0.03 K). Figure taken from *Ref.* [11].

Years later Stormer *et al*. [12] discovered that under very specific circumstances (very clean samples or high mobility) i can assume a series of fractional values. In this thesis we consider only the integer quantum Hall effect. To explain the quantization of the Hall resistance one usually thinks in terms of simple pictures that assume the effects of Anderson localization in strong magnetic fields. Most popular are Laughlin's gauge argument [13], the semi-classical percolation picture [14], the Landauer-Buttiker edge states picture [15] and the heuristic ideas on Anderson localization by Aoki and Ando [16] that are based on Kubo formula [17].

One way to realize the two dimensional electron gas (2DEG) is by making use of MOS field effect transistors (MOSFETs). Another way is to use GaAs/AlGaAs heterostructures [18] or GaAs/InGaAs quantum wells [11]. In MOSFETs one can easily change the electron density by changing the gate voltage. This is also possible in III/V heterostructures and

quantum wells, but easier than building an additional gate is to control the electron density by illuminating the sample at low temperatures (if the Hall bar has the property of persistent photoconductivity).

The breaking of translational invariance is due to ionized impurities or lattice impurities, both of which contribute to the disorder of the system. Anderson localization phenomena in perpendicular magnetic fields strongly depend on the *range* of the potential fluctuations. *Short-ranged* disorder gives rise to strong scattering between the electrons whereas *long-ranged* disorder is usually associated with semi-classical pictures where open orbits ("edge" states) percolate throughout the system. What determines the type of disorder in quantum Hall samples is the *range* of the potential fluctuations relative to the *magnetic length* $l_B = \sqrt{(\hbar/eB)}$. It is well known that in order to experimentally observe the *quantum critical* behavior of the quantum Hall plateau transition, short-range potential fluctuations should be prevalent.

1.3 Landau quantization

A major ingredient for the quantum Hall effect is Landau quantization. In absence of a magnetic field the density of states $N(E)$ (or DOS) of th e 2DEG is constant up to the Fermi level and given by [13]

$$N(E) = \frac{m^*}{\pi\hbar^2} \tag{1.3}$$

where m^* is the effective carrier mass. The Fermi energy (E_F) is given by

$$E_F = \frac{\pi n_e h}{m^*}, \tag{1.4}$$

where n_e is the 2DEG carrier density. Under influence of a magnetic field B directed perpendicular to the 2DEG the DOS splits up in a discrete set of Landau levels (*LL*s) per subband n with energies [19]

$$E_{n,s} = (l + \frac{1}{2})\hbar\omega_c + m_s g^* \mu_B B, \tag{1.5}$$

where l is an integer, m_s is the spin quantum number, g^* is the Landé-factor, μ_B is the Bohr magneton and ω_c is the cyclotron frequency:

$$\omega_c = \frac{eB}{m^*} \tag{1.6}$$

The second term in *Eq*. 1.5 accounts for the spin splitting. It follows from *Eqs* 1.5 and 1.6 that the energy distance between the *LL*s is proportional to the applied magnetic field *B*. In order to observe the quantum Hall effect the energy splitting of the *LL*s should be much larger than the thermal broadening of a single *LL*, $\hbar\omega_c >> k_B T$, which requires typically the experiments to be carried out at liquid helium temperatures ($T < 4$ K). The number of occupied *LL*s, *i.e.* the number of *LL*s with $E_{n,s} < E_F$ is called the filling factor ν. The filling factor ν is related to the magnetic field

$$\nu = \frac{hn_e}{eB} \tag{1.7}$$

By increasing the magnetic field, the Landau levels are successively pushed to above E_F, which gives rise – under quantum Hall conditions – to the plateau-plateau (PP) transitions (see Figure 2). When the Fermi level is located between two *LL*s R_H attains a plateau value and $R_0 = 0$. Ideally the quantum Hall transitions occur at filling factors (n + ½), where n = 0, 1, 2 etc. These are called the critical filling factors (ν_c). In practice however ν_c may slightly deviate from the ideal values due to a finite overlap of the *LL*s [11].

1.4 Plateau-insulator transition

The quantum Hall transition at the lowest Landau level at ν_c = ½ is a very special one. In the limit of large magnetic fields the 2DEG becomes an insulator with R_H quantized at the value of h/e^2 [20]. This transition has been termed the plateau-insulator (*PI*) transition. An example of magnetotransport data taken on an InGaAs/InP heterostructure in this regime are shon in *Fig* 1.3 [21].

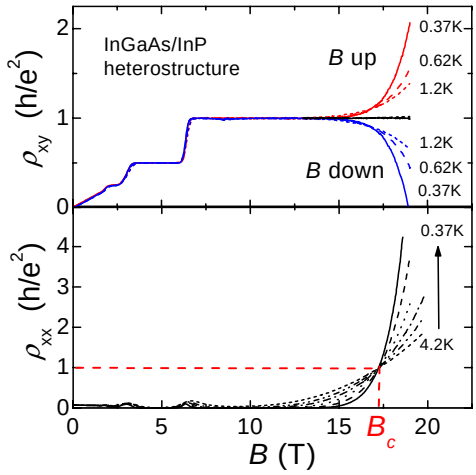

Figure 1.3 Magnetotransport data taken on an InGaAs/InP heterostructure ($n_e = 2.2 \times 10^{15}$ m^{-2}) covering PP transitions and the PI transition at $B_c = 17.2$ T. Upper frame: ρ_{xy} for positive and negative direction of the magnetic field B and the field-polarity averaged data. Lower frame: ρ_{xx}. Temperatures range from 0.37 to 4.2 K as indicated. Figure taken from *Ref.* [21].

The crossing point of the ρ_{xx} curves defines the critical field B_c at which the *PI* transition occurs. Due to sample inhomogeneities a sizeable component of ρ_{xx} is mixed into ρ_{xy} as seen in *Fig.* 1.3. However, by averaging over two polarities of the magnetic field ρ_H can be extracted from the ρ_{xy} data. An important feature to notice is that below the critical field B_c the longitudinal resistance decreases with decreasing temperature (metallic behavior) and above B_c the resistance increases with decreasing temperature (insulator type behavior). This is why often in literature this transition is referred to as a metal-insulator transition.

In this thesis we will focus on the plateau-insulator transition and extract the critical exponents of the quantum Hall quantum phase transition. The choice for the PI transition is motivated by the ability to deal with macroscopic sample inhomogeneities, which strongly affect the magnetotransport tensor and hamper a proper scaling analysis for the plateau-plateau transitions. This work strongly builds on the Ph.D thesis work of *Ponomarenko* [11] and *de Lang* [23].

1.5 Outline of this thesis

This thesis consists of seven chapters including this introduction.

In the second chapter several basic theoretical concepts relevant for the field of quantum phase transitions are introduced. We discuss scaling and power law behavior, and give the universal scaling functions for the conductivity tensor in the QHE. We illustrate relevant and irrelevant critical behavior with the help of a renormalization group flow diagram.
In Chapter 3 we present the experimental aspects of measuring the conductivity tensor on a Hall bar. We compare the commonly used AC-lock-in technique, with a newly implemented DC method, which we developed to reduce the effect of capacitive coupling for samples with very large resistance values. Sample details are also given in this Chapter.

In Chapter 5 we present a magnetotransport study on an InGaAs/GaAs quantum well in the quantum Hall regime. Data are taken at four carrier densities obtained by illuminating the sample. The PP-transition data are used to characterize the sample and determine the carrier density gradient of the Hall bar. The carrier density is evaluated with help of reflection symmetry and numerical simulations of the PP-transitions [11]. Next we investigate the longitudinal resistivity at the PI-transition and its critical behavior. The data are compared with previous results obtained on a different sized Hall bar [11]. Finally we report on a numerical study of the effect of the density gradient on the critical behavior of the PI transition for our specific Hall bar geometry.

Chapter 5 deals with the irrelevant critical behavior at the PI transition of the InGaAs/GaAs quantum well. We briefly discuss the concept of the "stress tensor" and distinguish between 'local' and 'global' variables. The ρ_H data are presented and analysed with a so-called data-collapse procedure, which gives access to the irrelevant critical exponent y_σ. Finally, we construct the renormalization group flow diagram and discuss its implications.

Chapter 6 deals with a different topic. Here we investigate the influence of a thin central AlAs barrier on the magnetotransport and optical properties of a δ-doped GaAs/InGaAs/GaAs quantum well. We first examine a series of six samples: three different pairs, each pair consisting of a sample with and without barrier. Magnetotransport data, photoluminescence data and wave function calculations are presented for the samples with and without barrier. It turned out that for this series of samples the δ-doping layers

themselves act as additional quantum wells and distort the shape and distribution of the wave functions. Therefore, a second series of samples was prepared and investigated.

In Chapter 7 again a new topic is introduced. Here we investigate the effect of a tilted magnetic field on an $In_xGa_{1-x}As/GaAs$ bilayer quantum well. In this material the Landé g-factor is much larger than the one in heterostructures that are traditionally used. This larger Landé g-factor will allow for a much larger spin splitting under influence of a magnetic field. Magnetotransport data in the quantum Hall regime for single (SQW) and double quantum wells (DQW) are presented and compared with each other. Several unique features in the data of the DQW system are explained using Landau level fan calculations.

1.6 References

[1] K.I. Wysokinski, *Eur. J. Phys.* **21** (2000) 535.

[2] A.M. Chang, H.D. Hallen, L. Marriott, H.F. Heu, H.L. Kao, J. Kwo, R.E. Miller, R. Wolfe, J. van der Ziel and T.Y. Chang, *Appl. Phys. Lett.* **61** (1992) 1974.

[3] L.D. Landau and E.M. Lifschitz, *Course in Theoretical Physics*, Vol. 8 (Pergamon Press, Oxford, 1984).

[4] A.A. Abrikosov, *Fundamentals of the Theory of Metals* (North-Holland, Amsterdam 1988).

[5] T. Ando, A.B. Fowler and F. Stern, *Rev. Mod. Phys*. **54** (1982) 437.

[6] K. von Klitzing, *Rev. Mod. Phys*. **58** (1986) 519.

[7] R.B. Laughlin, *Rev. Mod. Phys*. **71** (1999) 863.

[8] H.L. Störmer, *Rev. Mod. Phys*. **71** (1999) 875.

[9] D.C. Tsui, *Rev. Mod. Phys.* **71** (1999) 891.

[10] L. Bliek, E. Braun, F. Melchert, P. Warnecke, W. Schlapp, G. Weimann, K. Ploog, G. Ebert and G. Dorda, *IEEE Trans. Instrum. Meas*. **34** (1985) 304.

[11] L.A. Ponomarenko, *Ph. D Thesis* (University of Amsterdam, 2005), unpublished.

[12] D.C. Tsui. H.L. Stormer and A.C. Gossard, *Phys. Rev. Lett.* **48** (1982) 1559.

[13] R.B. Laughlin, *Phys. Rev. B* **23** (1981) 9375.

[14] J. H. Davies, *The Physics of Low-Dimensional Semiconductors*, (Cambridge University Press, Cambridge, 1998).

[15] M. Büttiker, *Phys. Rev. B* **38** (1988) 9375.

[16] H. Aoki and T. Ando, *Solid State Commun*. **38** (1981) 1079.

[17] R. Kubo, *J. Phys. Soc. Japan* **12** (1957) 570.

[18] T. Ando, A. B. Fowler and F. Stern, *Rev. Mod. Phys.* **54** (1982) 437.

[19] S. Datta, *Electronic Transport in Mesoscopic Systems* (Cambridge University Press, Cambridge, 1995).

[20] R.T.F. van Schaijk, A. de Visser, S. M. Olsthoorn, H.P. Wei and A.M.M. Pruisken, *Phys. Rev. Lett.* **84** (2000) 1567.

[21] D. de Lang, L.A. Ponomarenko, A. de Visser, C. Possanzini, S.M. Olsthoorn and A.M.M. Pruisken, *Physica E* **12** (2002) 666.

[22] D.T.N. de Lang, *Ph. D Thesis* (University of Amsterdam, 2005), unpublished.